California Polytechnic State University, San Luis Obispo

Winter Quarter 2019

THE TIMBER BUCKLING RESTRAINED BRACE FRAME

Senior Project Report prepared for:

Prof. Kevin Dong

Senior Project Report prepared by:

Jessica Resta

Senior Project sponsored by:

SSG Structural Engineers, LLP

ABSTRACT

With the increasing awareness on the topic of earthquake resistance, efficient, cost-effective, and environmentally friendly solutions in the structural field are on the rise. The purpose of this report is to investigate the Timber Buckling Restrained Brace (TBRB), a new lateral-resisting element made of steel and lumber, applicable in residential and small commercial units. In addition to the TBRBs' materials being readily available, the braces are easy to manufacture, reducing overall costs of production and transportation. The brace, made partly of wood, has also a low environmental impact when compared to other lateral force resisting elements like concrete shearwalls or steel moment frames. Members made of timber lack experimentations in new applications other than timber shearwalls, which are cost-effective solution only under low lateral force demands and when enough wall length is provided. The TBRB, exploring the combination of steel and a lumber casing, can achieve deformations and load demands in the ductile region of the steel that the timber shearwall can't.

LIST OF SYMBOLS

A_g = Gross crossectional area
B = Bay width
C_d = Deflection amplification factor
E = Modulus of elasticity
F_{cr} = Critical stress
F_e = Elastic buckling stress
F_y = Yielding stress
I_{xx} = Second moment of inertia about the x axis
I_{yy} = Second moment of inertia about the y axis
H = Story height
K_x = Effective length factor about the x axis
K_y = Effective length factor about the y axis
L = total length of element
L_x = Unbraced length about the x axis
L_y = Unbraced length about the y axis
P_{nx} = Nominal strength about the x axis
P_{ny} = Nominal strength about the y axis

b = Width of element
l = Yielding length of element
r_x = Radius of gyration about the x axis
r_y = Radius of gyration about the y axis
t = Thickness of element

Δ = Total brace deformation for the brace test
Δ_a = Allowable story drift
Δ_{bm} = Brace axial deformation corresponding to the inelastic story drift
Δ_{bx} = Brace axial deformation corresponding to the elastic story drift
Δ_d = Design story drift
ε = Strain
σ = Axial Stress

TABLE OF CONTENTS

1. PURPOSE

The purpose of this report is to investigate a new lateral force resisting system: the Timber Buckling Restrained Brace Frame (TBRB). The experiment involved determining the TBRB configuration, building four TRBR prototypes, and testing the prototypes through concentric cyclic loading of tension and compression. The expectation for the buckling restrained braced frame was of developing a ductile behaviour through cyclic loading of specified axial deformations.

2. INTRODUCTION

The TBRB ductility is achieved by an axially loaded steel core plate, restrained from compression buckling. The codified Buckling Restrained Brace Frame (BRB), a robust solution in high seismic regions, precedes the idea of the TBRB. The BRB is made of a steel core, restrained from lateral torsional buckling by a steel casing filled with grout (Figure 1). The BRB can dissipate large amounts of energy and reach the yielding zone in compression and tension loading of the core (Figure 2).

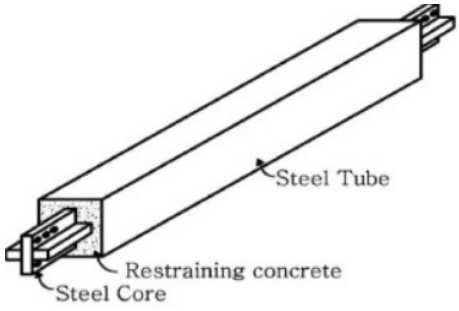

Figure 1: Buckling Restrained Brace

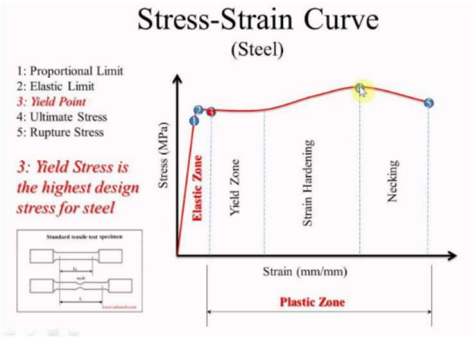

Figure 2: Stress-Strain Curve (Steel)

The BRB can reach higher ductile demands then the ordinary concentric brace frame (CBF), and this is demonstrated by the ability to sustain a stable balanced hysteresis curve under axial cyclic loading (Figure 3 and 4). The ability of the BRB to achieve uniform strains in tension and compression loading, while utilizing a small cross-sectional area of steel, relies on preventing core compression buckling. With the uniform core envelope of grout and steel, throughout the length of the casing the axially loaded core is braced about both the minor and major axis buckling effects.

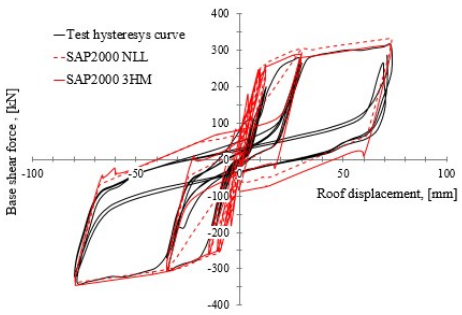

Figure 3: Hysteresis curve of the CBF

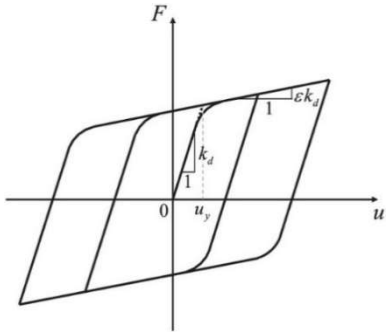

Figure 4: Hysteresis curve of the BRB

The BRB ductile behavior translates in a high response modification factor. Utilizing the equivalent static lateral force procedure (Section 12.14.8, ASCE 7-10), a high modification factor reduces the seismic base shear for the structure, making the BRB one of the most efficient lateral force resisting element.

3. DESIGN OF THE TBRB

The TBRB is made of a steel core plate and a casing of timber and flat bars for lateral torsion buckling restraints (Figure 5, left). The key of using a brittle material to prevent buckling is to design the brace such that no force transfer occurs from the core to the casing; the configuration is designed for the core to be the only material axially deforming and dissipating energy. The TBRB configuration is designed for an adequate gap between the steel, the wood edge, and the welded plates, allowing for the ductile deformation of the axial core plate. Additionally, there is no positive connection between the core and the restraining elements, and the assembly relies on friction to not slip, causing the casing to move independently during the loading of the core plate.

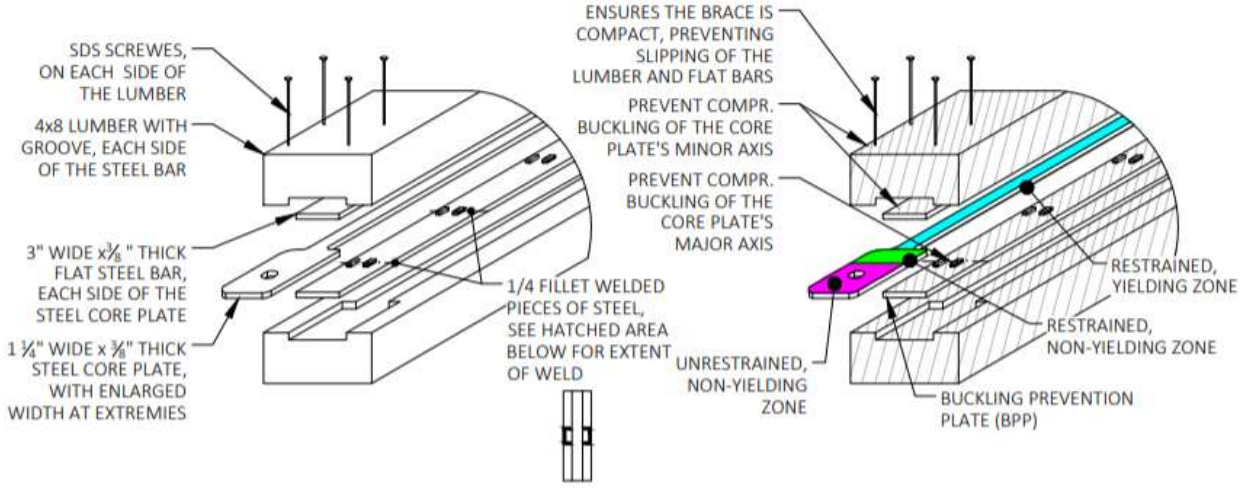

Figure 5: TBRB apparatus, to the left, and function of materials, to the right

3.1 COMPRESSION BUCKLING

The flexural buckling and yielding forces for the TBRB prototypes were calculated following the AISC 360 requirements for compression loading without slender elements (section E3). The equations used are shown below, and the cross-sectional properties and material yield strength of the tested core are shown on the next page (Table 1).

1) Nominal Compressive Strength [E3-1, AISC 360]:

$$P_n = A_g * F_{cr}$$

2) Critical Stress for Inelastic Buckling $\left(F_y/F_e \leq 2.25\right)$ [E3 − 2, AISC 360]:

$$F_{cr} = \left[0.658^{F_y/F_e}\right] * F_y$$

3) Critical Stress for Elastic Buckling $\left(F_y/F_e > 2.25\right)$ [E3-3, AISC 360]:

$$F_{cr} = 0.877 * F_e$$

4) Elastic Buckling Stress [E3-4, AISC 360]:

$$F_e = E * \pi^2/(KL/r)^2$$

Table 1: Cross-sectional properties and material yield strength of TBRB core plate

t	0.375	in
b	1.25	in
L	92	in
A_g	0.46875	in^2
F_y	44	ksi
E	23307	ksi

The TBRB compression buckling restraints are nonuniform about the core's axis (Figure 5, right), therefore the analysis of the core behaviour under compression loading differs about the minor and major axis.

Minor axis compression buckling prevention

The steel buckling prevention plates (BPPs) and timber members provide continuous bracing within the restrained yielding and non-yielding zone of the core (green and cyan highlight, Figure 5). The bracing from the lumber and BPPs prevents the effects of Euler Buckling's curve to govern the yielding behaviour about the minor axis (Figure 6). During loading, the out-of-plane core deflection during compression show in Figure 7 induces stresses on the lumber casing. The BPPs are a necessary element for the lumber to sustain the brace deformation without crushing, a failure largely due to the use of solid sawn lumber rather than a heavy timber with higher stress capacities. By increasing the area of stress distribution with the application of the BPPs, the lumber is able is to resist the stress from core plate buckling about the minor axis.

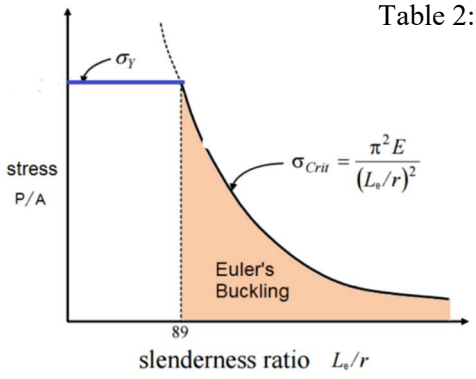

Figure 6: Euler's Buckling Curve

Table 2: Compression strength of the core plate about the minor axis

Minor Axis Compression Yielding	
I_{yy}	0.00549 in^4
K_y	1
L_Y	0 in
$K_Y L_Y$	0 in
r_Y	0.1083 in
$(KL/r)_Y$	0
F_e	0, ksi
F_y/F_e	0.000 no buckl.
$F_{cr}(ksi)$	44.00 ksi
$P_Y(kips)$	**20.63** $kips$

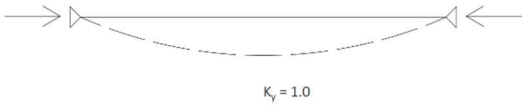

Figure 7: Predicted deflected shape and effective length factor about the minor axis

Major axis compression buckling prevention

Due to the assembly of the TBRB, compression loading inhibits Euler's buckling effects about the major axis of the core. To prevent the lateral torsional buckling failure modes, steel plates are welded to the BPPs, reducing the unbraced length of the major axis. The welded plates assembly results in two different unbraced lengths analysis for the core plate: pin-pin and fix-free (Figure 8). The pin-pin condition is

between the welded plates, with an effective length factor of 1.0, while the fix-free condition is between the extreme welded plates and the bolted connection, with a factor of 2.0. The governing effective length factor is the fix-free behavior, due to the unbraced length being doubled.

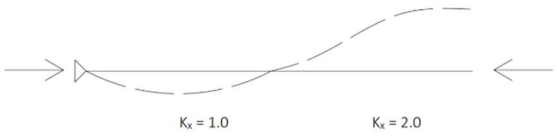

Figure 8: Effective Length Factor

Table 3: Compression strength of the core plate about the major axis

Major Axis Compression Buckling (Fix-Free)		Major Axis Compression Buckling (Pin-Pin)	
I_{xx}	0.06104 in^4	I_{xx}	0.06104 in^4
K_x	2	K_x	1
L_x	11.25 in	L_x	12.4 in
K_xL_x	22.5 in	K_xL_x	12.4 in
r_x	0.3608 in	r_x	0.3608 in
$(KL/r)_x$	62.35	$(KL/r)_x$	34.36
F_e	59.17 ksi	F_e	194.80 ksi
F_y/F_e	0.744 inelastic buck.	F_y/F_e	0.226 inelastic buck.
$F_{cr}(ksi)$	32.23 ksi	$F_{cr}(ksi)$	40.03 ksi
$P_{nx}(kips)$	**15.11** $kips$	$P_{nx}(kips)$	**18.76** $kips$

By comparing the compression capacities about the minor and major axis from Table 2 and 3, it is inferred that the governing buckling failure mode for the TBRB is the fix-free condition about the major axis. The location of the extreme plates, as well as the welding, are critical elements of the TBRB design.

3.2 STORY DRIFT REQUIREMENTS

The story drift requirement for the prototypes met the protocol of AISC 341 for buckling-restrained braced frames (Section K3-4c). The provisions of AISC require a minimum design deformation for a drift of 1% the height of the story. The design story drift for the prototypes tested was calculated as a 75% reduction of the allowable story drift, defined in ASCE 7-10. The reduction of the design story drift is compatible with the allowable capacities of the compression buckling restraints, and it overall reduces the forces demanded on the frame assembly.

5) Allowable Story Drift [Risk Category II, T.12.12-1, ASCE 7-10]:

$$\Delta_a = 0.020 * H$$

6) Design Story Drift:

$$\Delta_d = 0.0125 * H$$

The design story drift was determined by the proportion of a 20'x12' frame, and the brace displacement, Δ_{bm}, was found by applying trigonometry on the basis of small angles theory. Refer to Figure 9 for the diagram of the frame analyzed to determine the story drift and brace deformation shown in Table 4.

7) Brace deformation based on design story drift:

$$\Delta_{\text{bm}} = \Delta_d * \cos\theta$$

Table 4. Deformation demand by proportion

Allowable Story Drift 20'x12' Frame		Proportion for Protype	
H	12 ft	l_{TOT}	7.67 ft
B	20 ft	l	7.08 ft
L	23.32 ft	Δ_{bm}	0.507 in
Δ_a (2%H)	0.24 ft		
Δ_d (1.25%H)	0.15 ft		
Δ_{bm}	1.543 in		

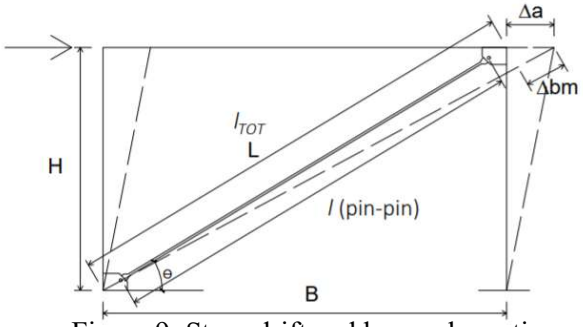

Figure 9: Story drift and brace elongation

Note that for a codified lateral force resisting element, the inelastic design story deformation is calculated as an amplification of the elastic deformation.

8) Inelastic brace axial deformation (the importance factor has been omitted) [12.8-15, ASCE 7-10]:

$$\Delta_{bm} = C_d * \Delta_{bx}$$

9) Brace elastic axial deformation (utilizing the values from Table 1):

$$\Delta_{bx} = {}^{P_y * l}/_{E * A} = \ 0.1605\ in\ (for\ the\ protoypes)$$

Based on the elastic axial deformation Δ_{bx} and the required brace deformation for the test specimens Δ_{bm}, the TBRB value for C_d is equal to 3, which would be an adequate value compared to the common ones for lateral force resisting elements. The greatest deflection amplification factor in the ASCE 7-10 is equal to 6, and the BRB value for C_d is equal to 5. A greater amplifications factor corresponds to a greater inelastic story drift capability, which equates to larger amounts of energy dissipated in the lateral force resisting element.

3.3 DEFORMATION REQUIREMENTS

The loading protocol for testing the four TBRB prototypes followed the requirements specified in ASCE 341 (Section K3-4c). The testing requires controlled levels of axial or rotational deformation for the test specimen, Δ_{bm}. The loading sequence must be of 5 specified steps, each composed of 2 cycles of axial loading (1 cycle defined as one loading in tension and one loading in compression). An additional step is required to achieve a cumulative inelastic deformation of at least 200 times the yield deformation.

The test on the TBRB specimens was conducted by imposing the required axial deformation loading sequence on the braces. The axial deformation loading, the predicted force on the prototypes, and the loading rate of the experiment are summarized in Table 5.

Table 5. Cyclic loading and predicted demand on the brace

Step	Demand	Cycles	Δ	Load rate (in/min)	ε (in/in)	σ (ksi)	P (kips)
1	Yield	2	0.1604	0.375	0.00189	44.00	20.63
2	$0.5*\Delta_{bm}$	2	0.2348	0.500	0.00276	44.62	20.92
3	$1.0*\Delta_{bm}$	2	0.4697	0.750	0.00553	46.62	21.85
4	$1.5*\Delta_{bm}$	2	0.7045	1.000	0.00829	48.62	22.79
5	$2.0*\Delta_{bm}$	2	0.9393	1.000	0.01106	50.62	23.73
6	$1.5*\Delta_{bm}$	2	0.7045	1.000	0.00829	48.62	22.79

The loads predicted in Table 5 were obtained by testing dog-bone shaped specimens made from the same material as the core plate. The specimens were tested through tensile axial loading, and strain was recorded with the use of an extensometer (Image 1, next page). The stress-strain graph of one specimen is plotted in Figure 10, utilizing the 0.002 strain offset yield method (Section K3-6b, AISC 341).
The results of yield strength and modulus of elasticity from the sheet of steel used for fabrication indicated it was not A36, the preferred material specified per the ASTM provisions. Rather, due to the yielding stress being equal to 44 ksi, the core was manufactured from a high-strength low-alloy sheet of steel.

Image 1: Strain-gage testing

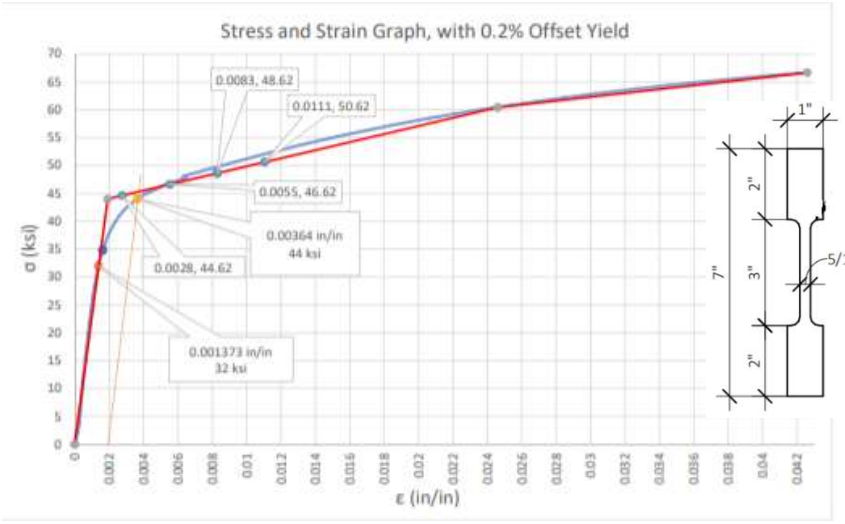

Figure 10: Stress and strain graph and tested dog-bone specimen

3.4 CONNECTION REQUIREMENTS

Since the TBRB specimens were not tested in a frame assembly, the connection was manufactured specifically for the testing machine used, and it was designed by a previous group testing the TBRB specimens in 2018. The connection is composed by a 1" diameter A3250 bolt and 2- ¼" thick vertical plates. The vertical plates are welded to the horizontal plate, and a 1½" threaded rod is welded in the center of the base plate (Figure 11 and Image 2); the rod is then fastened to the machine with a hexagonal nut. The connection components were designed per AISC requirements (Section J) and Load and Resistance Factor Design (LRFD); the failure mode analyzed were:

- Yielding capacity of the plates and rods;
- Strength of fillet welds;
- Block shear of the core plate;
- Shear strength of bolt.

Image 2: Top connection of the brace

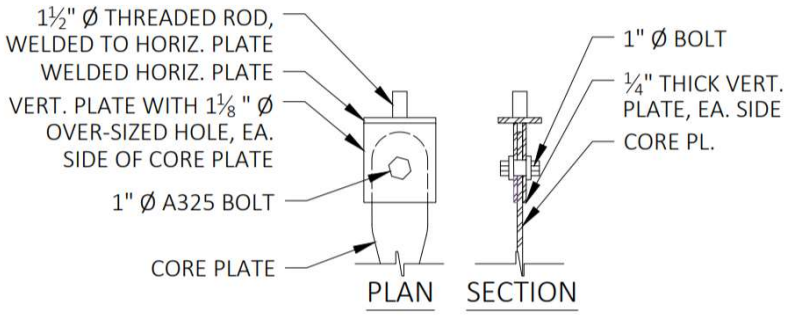

Figure 11: TBRB connection

4. TESTING THE TBRB

The brace test specimens replicated the construction features and material properties of the TBRB. Pictures of the specimens before testing are shown below in Image 3.

Image 3: Pictures of TBRB assembly before testing

For testing, the brace was connected at the top of the machine and then lifted to allow for the bottom pin connection to be fixed (Image 4). Note that the force on the machine was set to zero after the brace was installed, therefore the compression and tension axial forces measured do not account for the self-weight of the brace. Utilizing the typical specific weight densities of 33 lbf/ft^3 for wood and 490 lbs/ft^3 for steel, the brace self-weight was of approximately 150 pounds, with weight varying based on moisture content of the lumber.

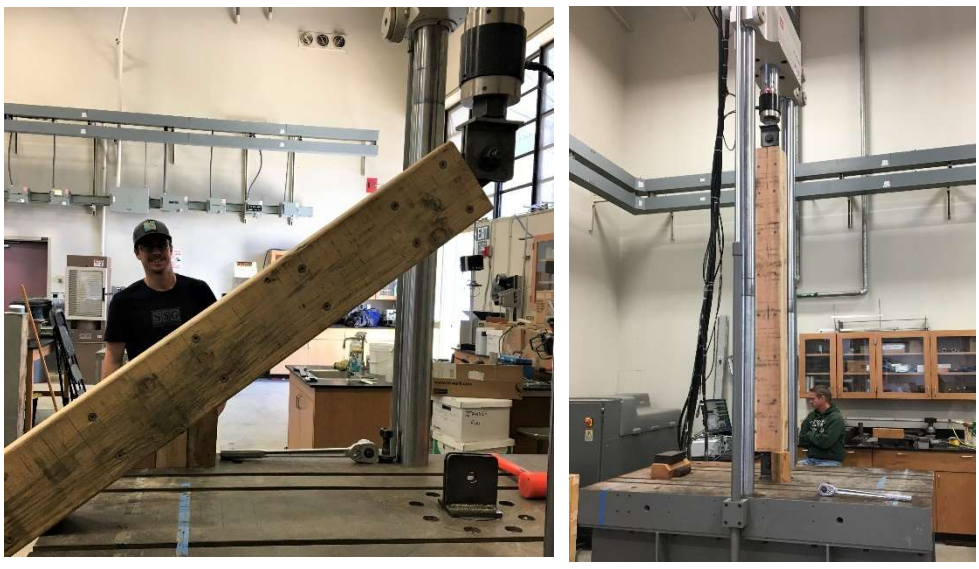

Image 4: Pictures of TBRB installation

During installation on the testing machine, the lumber casing and steel plates shifted downwards, changing the position of the buckling prevention restraints. To address the sliding of the steel plates (BPPs), copper straps were screwed to the bottom end of the lumber pieces; while for the wood casing, blocking was used to prevent sliding. The sliding prevention mechanisms resulted in a much better behaviour of the braces, and it was implemented after the first specimen was tested. The installation of the components is illustrated below.

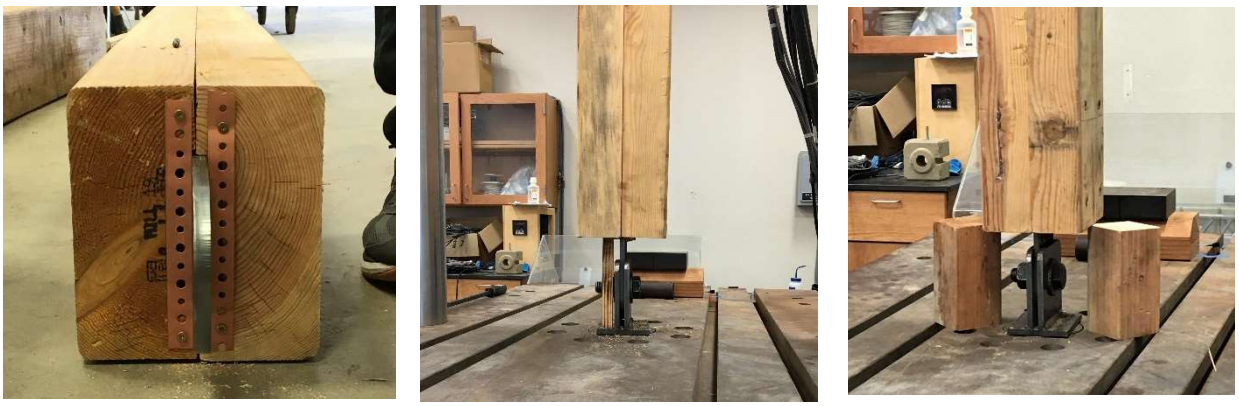

Image 5: Pictures of sliding prevention for the TBRB: for the BPPs, left, and for the casing, right.

The critical failure modes were consistent throughout the tests:

1) Buckling of the unrestrained non-yielding zone of the core plate (refer to Figure 4);
2) Splitting of the lumber due to out-of-plane buckling of the core plate

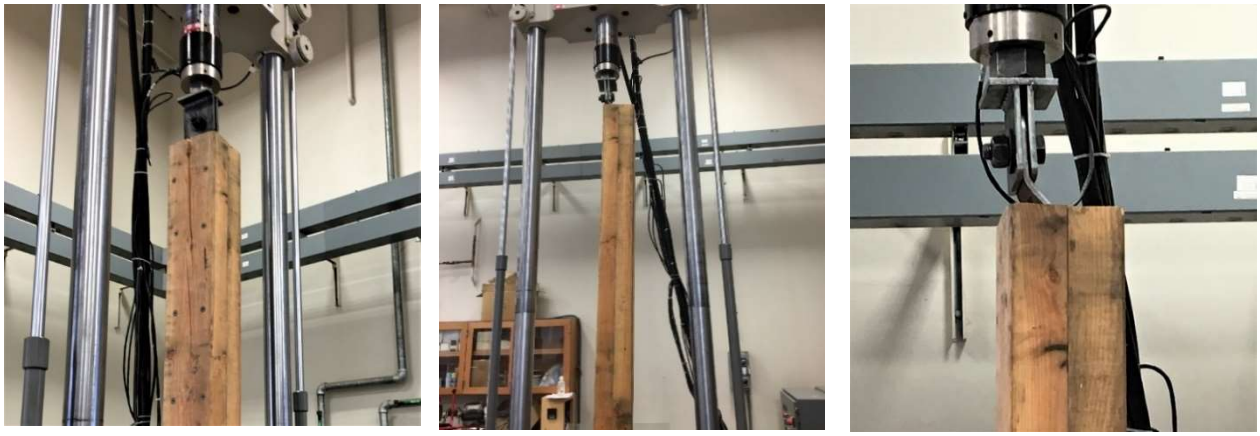

Image 6: Pictures of buckling deformation, wood splitting, and connection deformation during testing

As shown in Image 6, during testing, the unrestrained zone of the core (pink highlight, Figure 5) buckled about the minor axis, causing the deformation of the horizontal plates of the connection assembly. The deformation in the connection increased with loading, inhibiting buckling effects in the top connection of the brace for all specimens.

Buckling in the non-restrained zone and the yielding behaviour of the restrained zone of the core plate are shown in Image 7 and 8, which are pictures of the specimens after loading.

Image 7: Buckling of non-restrained zone. The left picture is of the bottom undeformed connection of the brace, the middle and right pictures are of the top deformed connection of the brace.

Image 8: Yielding of the core plate (Specimens #2, #3, and #4), and buckling, right top image; Note that the welded plates did not displace or rotate during testing.

4.1 RESULTS

The axial deformation and corresponding axial force on the braces were recorded during the concentric loading tests. The maximum force reached per each step and the hysteresis curves from the four tests specimens are shown in Figure 11 to 14.

Brace #1 was not connected tightly enough to the bottom of the machine, and testing had to be interrupted during the end of the second cycle of step 4, $\Delta = 0.705$". In addition, no wood blocking was in place for the first testing, and the casing was sliding, affecting the core buckling behaviour.

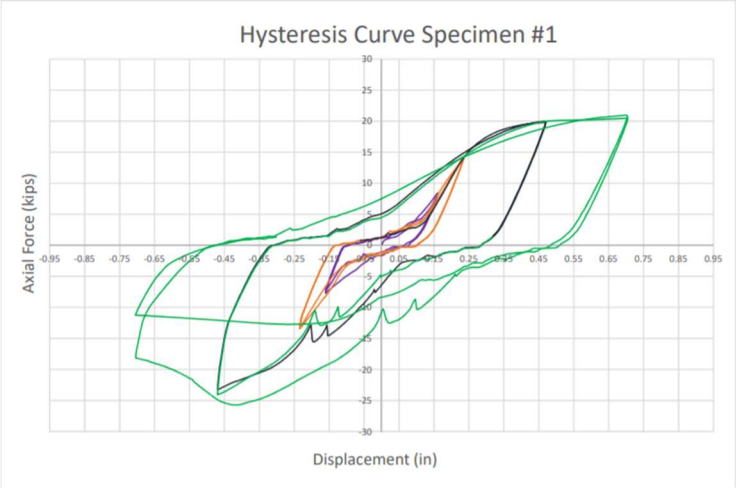

Specimen #1			
Step	Δ (in)	T (lbs)	C (lbs)
1	0.160	8,500	7,750
2	0.235	14,010	13,492
3	0.470	19,809	23,303
4	0.705	20,962	25,731
5	0.940	--	--
6	--	--	--

Figure 11: Tested Brace #1 and maximum recorded axial force

Brace #2 was loaded at the maximum deformation of $\Delta = 0.94$" (Step 5) only in the tension loading cycle. Figure 12 shows the high compressive force dissipated by the core during Step 4, and testing was interrupted due to the wood crushing and the minor axis buckling effect in the unrestrained zone of the core.

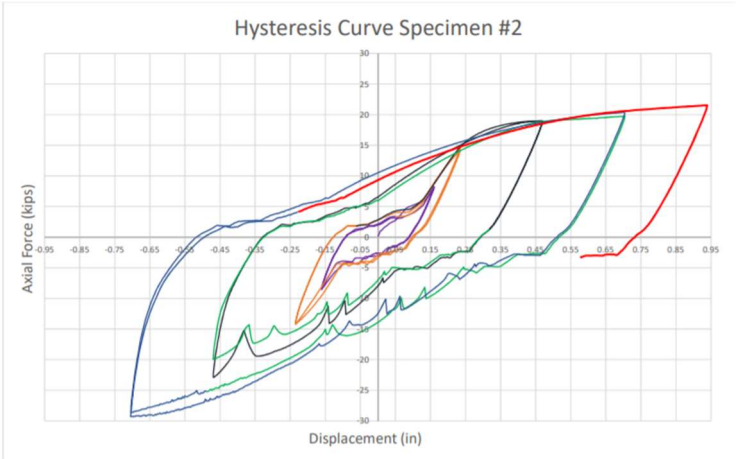

Specimen #2			
Step	Δ (in)	T (lbs)	C (lbs)
1	0.160	8,313	8,550
2	0.235	14,615	14,351
3	0.470	18,978	22,941
4	0.705	19,754	29,338
5	0.940	21,533	--
6	--	--	--

Figure 12: Tested Brace #2 and maximum recorded axial force

Brace #3 dissipated the most amount of energy. The specimen achieved the maximum deformation of $\Delta = 0.94$" for the two cycles of compression and tension loading (shown in red). As shown in Figure 13, during Step 5, specimen #3 reached a compressive force of 29,703 pounds and a tension force of 23,099 pounds. The tension force for Step 5 was close to the predicted axial load from the dog-bone specimen recorded in Table 5. Brace #3 was additionally deformed through Step 6, which corresponded to a deformation of $\Delta = 0.70$" (shown in dashed red). During Step 6, the Brace experienced a reduction of compression force of 12 compared to Step 4, where the core was loaded for the same deformation. The drop in axial force indicates a loss of strength in the core due to the permanent deformation during compression loading and reduction of cross-sectional area during tensile loading.

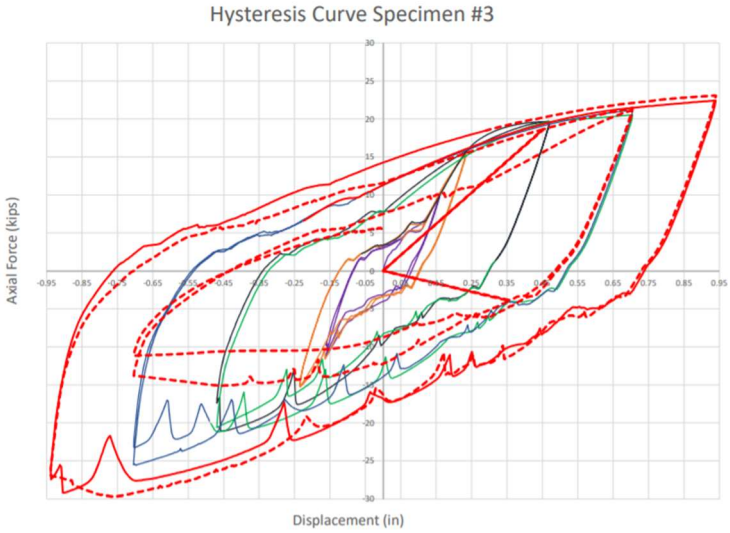

Specimen #3			
Step	Δ (in)	T (lbs)	C (lbs)
1	0.160	10,203	11,153
2	0.235	15,668	15,325
3	0.470	19,690	21,101
4	0.705	21,163	25,605
5	0.940	23,099	29,703
6	0.705	21,449	13,843

Figure 13: Tested Brace #3 and maximum recorded axial force

Brace #4 was also able to undergo the maximum deformation for both the cycles of compression and tension loading. The brace also resulted in the lowest axial force in the core plate and the least difference between tensile and compressive force. In fact, during Step 5, the difference between tensile and compressive force in Brace #4 was of only of 6%, and the maximum compressive force reached, about 23 kips, was 26% lower than in Brace #3, which experienced 29.7 kips of compressive force.

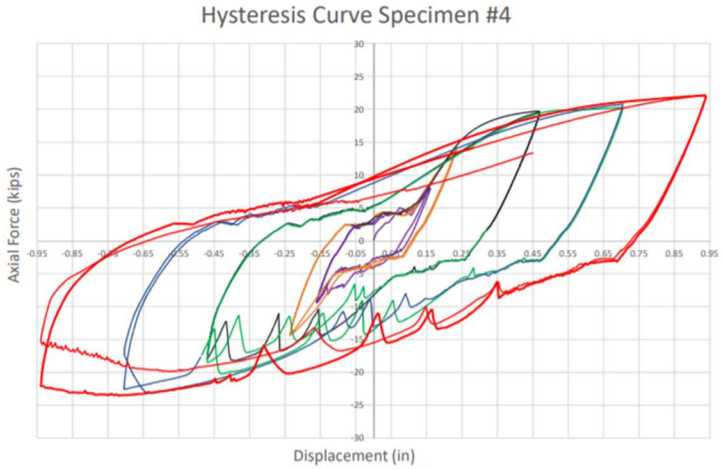

Specimen #4			
Step	Δ (in)	T (lbs)	C (lbs)
1	0.160	8,890	9,484
2	0.235	14,484	14,382
3	0.470	19,713	18,566
4	0.705	20,771	23,150
5	0.940	22,139	23,554
6	--	--	--

Figure 14: Tested Brace #4 and maximum recorded axial force

4.2 DISCUSSION

The results from testing the TBRBs indicate that two braces (#3 & #4) were able to reach the maximum design deformations specified in the steps of Table 5. Although the wood was crushing and the extreme edges of the core buckled, the braces were able to achieve yielding behaviour in the tension and compression zone. It must also be noticed that yielding in the brace started occurring after the third step, with 0.25" axial deformation. The yield strain predicted for the core was of .19%, but the tested value was rather of .55% strain. Also, all braces experienced compression overstrength effects due to the molecular structure of the material under compression loading.

The discussion of the performance during testing and the methods to improve the TBRB behaviour lies in the understanding of the core compression lateral torsional buckling prevention and the BPP and lumber casing slipping prevention.

Slipping behaviour

Due the TBRB assembly relying on friction, the loaded casing is induced to slip for the weight of its components and the applied compression force. The assembly of the brace must be very tight, and it is advised during manufacturing to hammer the buckling prevention plates in the wood casing. For the tested TBs, pieces of wood with small cross-sectional area were used to prevent slipping, as the casing was bearing on it. The bearing area was reduced to a minimum in order to not affect the compression results of the specimens (Image 5). To prevent the whole case from slipping, a bearing condition that also allows the core plate to deform must be implemented. An option might be to increase the width of the core and drill a minimum number of oversized holes, which would allow for deformation of the core and bearing of the casing (Figure 15).

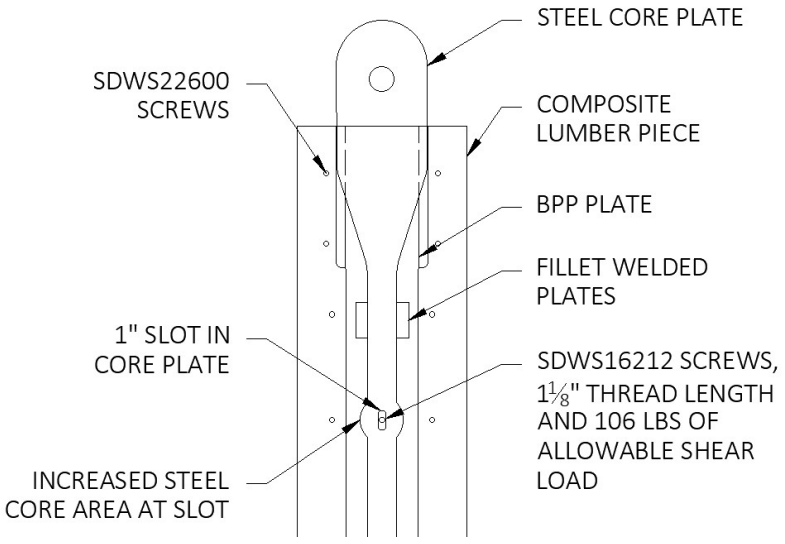

Figure 15: Plan view of proposed TBRB assembly

Major Axis Behaviour

The major axis predicted behaviour was of Euler's buckling demand to govern (Table 3), but the results showed the core was restrained by buckling, inducing yielding behaviour (Image 8). The major axis was partly restrained by the use of blocking during testing. By preventing sliding, the unbraced length of the fix-free condition was not increased. But the success of the core plate yielding was largely due to the welded plates connections. The connections showed a pin-pin behaviour, as no major rotation effects were witnessed after testing. The 12" spacing of the plates and the detailed fillet welds reduced the overall buckling force on the major axis, preventing the fix-free condition at the extremities of the brace to govern.

Minor Axis Behaviour

The buckling failure shown in Image 7 was in the unrestrained zone of the minor axis, and it was due to the distance between the bolted connection and the wood member. The gap was conservatively designed and manufactured as 3 times the maximum design deformation reached in Step 5. But the results indicated that a less conservative design would have prevented the buckling mechanism to take place. Although the buckling behaviour of the unrestrained zone of the core occurred, the brace was able to reach the predicted yielding behaviour in the restrained zone of the minor axis, and it was not affected by Euler's buckling curve. During testing, the wood for all four specimens started splitting at the 0.70" deformation (Image 6). The stress transfer from the axial deformation of the core caused the wood member to split, therefore it is advised to use a stiffer timber member such as a composite lumber.

5. CONCLUSION

The TBRB's results from axial concentric loading showed a ductile behaviour for the braces, and the testing expectation of reaching inelastic strains in tension and compression cycling loading were achieved. With the steel core plate yielding, buckling prevention was overall successful, and the design brace deformations were reached for most of the specimens. Studying the effects of loading on the prototypes tested informs on methods to improve the ductility of the TBRB and prevent modes of failure. This experiment proves the potential of incorporating the TBRB as a ductile lateral force resisting element for structures to withstand earthquake forces.

6. FABRICATION OF THE TBRB

- SDWS22600DB Simpson strong-tie screws (Impact drill is recommended)
- 1 sheet of 48”x96”x ⅜” hot-rolled, low carbon Steel
- 8 pieces of 8’-0” long, 4x8 DF #1 Lumber
- 2 flat bars 20’-0” long, 3”x ⅜ hot-rolled Steel
- 2 flat bats 10’-0” long. 3” x ¼” hot-rolled Steel
- Wood Surface Planer
- Compound Miter Saw
- CNC router
- Plasma cutter
- Cold Saw
- MIG welding equipment
- ⅛” diameter, 4” long or more, drill bit and drill

CONSTRUCTION PROCESS

Wood:

1. Plane the surface of the wood that will be in contact with the steel.
2. Use the miter saw to cut the wood to length, 6’-8” long.
3. Use the CNC router to create the lumber groove for the wood and provide a correct Rhino Cam drawing.
    - Measure the wood and steel true cross-sectional dimensions
    - Consider a tolerance of ⅛” for the width and 1/16” for the depth of the lumber groove
    - Provide continuous blocking for the lumber during the routing process.

Steel:

1. Use the Plasma cutter and the AutoCAD profile to cut out the steel shape for the core.
2. Use the cold saw to cut the flat bars to length, 6’-8” long.
3. From the sheet of steel remaining, use the cold saw to cut ½”x1 ½” small pieces of steel.
4. Fillet weld the small pieces of steel to the flat bars, leaving a small gap from the edge of the core.
    - Clamp the core to the flat bar while welding, to ensure a tight fit.
    - Position the plates at the designed spacing, and tap weld the two edges first.
    - Pay attention to not weld any material on the steel core; and if there is a welded connection, use a metal grinder to remove it.

Consider pre-drilling holes on the wood, so you can use the long drill bit to mark the location of the screws on the side of installation. Use a router, a jig, and a rabbit planer to remove any additional wood material for ease of installation and correct manufacturing of the specimen.

CONSTRUCTION PICTURES

CNC Milling of the lumber casing

Plasma cutting the core plates

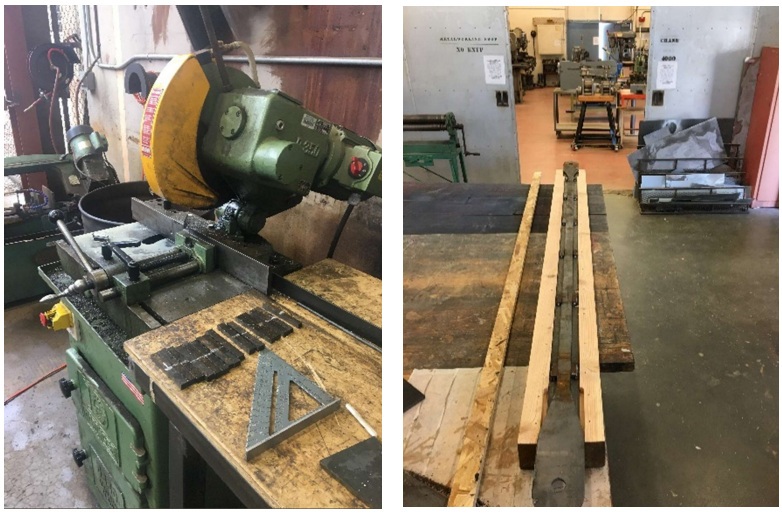

Cutting the welded plates and assembling the brace